POLITECNICO
MILANO 1863

SCUOLA DI INGEGNERIA INDUSTRIALE
E DELL'INFORMAZIONE

In-depth analysis for the course Fundamentals of Hypersonic flows

A review on chemical-kinetic models for hypersonic flows in thermo-chemical nonequilibrium

Laurea Magistrale in Aeronautical Engineering

Author: Federico Cutolo

Person code: 10521274

Advisor: Prof. Giulio Gori

Academic year: 2022-2023

Abstract

The conservation equations for simulating hypersonic flows in thermal and chemical nonequilibrium for the Air-11 model are presented. The chemical-vibrational coupling is introduced with Park's two-temperature model, together with its reaction set and kinetic parameters. Park's model of 1987 is compared with the models of Park 1991, Gupta, Dunn-Kang. The comparison is based on a numerical study of the heat flux on the surface of the Apollo command module at $Ma = 20.5$. The differences between the models are ascribed to the difference in reaction rates involving N_2 and O_2.

1. Introduction

Re-entry vehicles in hypersonic high enthalpy re-entry flows encounter thermochemical nonequilibrium states (Fig.8). Nonequilibrium processes occur in a flow when the time required for a process to accommodate itself to local conditions within some region is of the same order as the transit time across that region. If the accommodation time is very short compared with the transit time, the process is in equilibrium. If the accommodation time is very long compared with the transit time, the process is frozen. The length scale of the region depends on what is being studied. A useful length scale could be the shock stand-off distance. The ongoing process can be a chemical reaction or an exchange in energy between energy degrees of freedom (translational, rotational, vibrational, electronic).
In the Air-11 model, the accommodation process takes place with collisions of heavy particles (molecules, atoms, ions) among themselves or with electrons. The accommodation time is given by the frequency of the collisions. Even though the collision rate might be high enough to keep the velocity distribution functions close to the equilibrium (Maxwellians), the number of effective collisions, in terms of vibrational energy transfer or chemical reaction, might be much smaller. In this case, the vibrational or chemical relaxation is not fast enough to keep the local thermochemical equilibrium. Hence, it is necessary to model vibrational and chemical kinetics in a coupled fashion to prescribe accurate chemical rate coefficients and, ultimately, attain a precise description of the heat flux around the body.

2. Conservation Equations

High-temperature air is assumed to be composed of the following 11 species: N_2, O_2, N, O, NO, N_2^+, O_2^+, NO^+, N^+, O^+, e^-. The conservation equations for a reacting gas flow in which thermal nonequilibrium is modeled with a three-temperature approximation (i.e., three-energy equations) can be expressed as follows.

Species conservation:

$$\frac{\partial \rho_s}{\partial t} + \frac{\partial \rho_s u^j}{\partial x^j} = \frac{\partial}{\partial x^j}(\rho D_s \frac{\partial y_s}{\partial x^j}) + \dot{w}_s \tag{1}$$

Mixture Momentum conservation:

$$\frac{\partial}{\partial t}\rho u^i + \frac{\partial}{\partial x^j}\rho u^i u^j = -\frac{\partial p}{\partial x^i} + \frac{\partial}{\partial x^j}\left[\mu\left(\frac{\partial u^i}{\partial x^j} + \frac{\partial u^j}{\partial x^i}\right) - \frac{2}{3}\mu\frac{\partial u^k}{\partial x^k}\delta^{ij}\right] \tag{2}$$

The pressure p is defined as

$$p = \sum_{s=1}^{11} p_s \tag{3}$$

and the partial pressure of species s is defined by

$$p_s = \frac{\rho_s \bar{R} T}{M_s} \tag{4}$$

Where M_s is the molecular weight of species s, and $\bar{R}$ is the universal gas constant. μ is the mixture viscosity.

Vibrational Energy conservation

$$\frac{\partial}{\partial t}\rho e_v + \frac{\partial}{\partial x^j}\rho e_v u^j = \frac{\partial}{\partial x^j}\left(\eta_v \frac{\partial T_v}{\partial x^j}\right) + \frac{\partial}{\partial x^j}\left(\rho \sum_{s=1}^{11} h_{e,s} D_s \frac{\partial y_s}{\partial x_j}\right) + \dot{Q}_{v-t} + \dot{Q}_{v-e} + \sum_{s=1}^{N_{mol}} \dot{w}_s \hat{D}_s \tag{5}$$

Were the vibrational energy per unit mass e_v is defined as:

$$e_v = \sum_{s=1}^{11} \frac{\rho_s e_{v,s}(T_e)}{\rho}$$

The second term of the right-hand side is the conduction of vibrational energy across the control volume due to vibrational temperature gradients. The third term of the right-hand side represents the diffusion of vibrational energy due to concentration gradients. $\dot{Q}_{v-t}$ and $\dot{Q}_{v-e}$ are the rate of energy exchange between vibrational and translational modes and between vibrational and electronic modes due to collisions within the volume, respectively:

$$\dot{Q}_{v-t} = \sum_{s=1}^{N_{mol}} \rho_s \frac{(e^*_{v,s} - e_{v,s})}{< \tau_s >}$$

$$\dot{Q}_{v-e} = \sum_{s=1}^{N_{mol}} \rho_s \frac{(e^{**}_{v,s} - e_{v,s})}{< \tau_{es} >}$$

Where $e^*_{v,s}$ and $e^{**}_{v,s}$ are the vibrational energy of species s evaluated at the roto-translational temperature and electronic temperature respectively, while $e_{v,s}$ is the total vibrational energy associated with the species. The last term accounts for the vibrational energy loss or gain due to chemical reactions of dissociation and recombination respectively. $\hat{D}_s$ is the vibrational energy per unit mass of the diatomic molecules, created or destroyed at a rate $\dot{w}_s$.

Electron and Electron Excitation Energy conservation:

$$\frac{\partial}{\partial t}\rho e_e + \frac{\partial}{\partial x^j}\left[u^j(\rho e_e + p_e)\right] = u^j \frac{\partial p_e}{\partial x^j} + \frac{\partial}{\partial x^j}\left(\eta_e \frac{\partial T_e}{\partial x^j}\right) + \frac{\partial}{\partial x^j}\left(\rho \sum_{s=1}^{11} h_{e,s} D_s \frac{\partial y_s}{\partial x^j}\right) + \dot{C}_{h-e}(T_e) + \dot{Q}_{v-e} - \dot{I}^e - \dot{Q}_{rad} \tag{6}$$

Where the terms of the left-hand side represent the rate of change of electronic energy per unit volume in a cell-centered at x^j and the flux of electronic enthalpy across cell walls with velocity u^j. In particular

$$e_e = \sum_{s=1}^{11} \frac{\rho_s e_{e,s}(T_e)}{\rho}$$

The first term on the right-hand side represents the work done by electrons subject to electron pressure gradients. $\dot{C}_{h-e}(T_e)$ is the energy exchange due to collision between heavy particles and electrons. $\dot{Q}_{v-e}$ is again the rate of energy exchange between electronic and vibrational modes. $\dot{I}^e$ embeds the energy loss due to ionization of molecules and atoms, where electrons are lost. $\dot{Q}_{rad}$ represents the rate of energy loss due to radiation, where electrons

transit from upper to lower energetic levels.

Total Energy conservation

$$\frac{\partial}{\partial t}\rho E + \frac{\partial}{\partial x^j}\rho H u^j = \frac{\partial}{\partial x^j}\left(\eta\frac{\partial T}{\partial x^j} + \eta_v\frac{\partial T_v}{\partial x^j} + \eta_e\frac{\partial T_e}{\partial x^j}\right) + \frac{\partial}{\partial x^j}\left(\rho\sum_{s=1}^{11} h_s D_s \frac{\partial y_s}{\partial x^j}\right) + \dot{S} + \dot{Q}_{rad} \quad (7)$$

The total energy is defined as

$$E = \frac{1}{2}u^i u^i + \sum_{s=1}^{11}\frac{\rho_s e_s}{\rho}$$

while the total enthalpy is defined as

$$H = E + \frac{p}{\rho}$$

$\dot{S}$ represents the work done by shear forces. The conservation equations were taken from [11].

3. Two-temperatures model

The three-temperatures model used to define the equations 1-7 considers the partitioning of energy among the modes can be described by three temperatures T, T_v and T_e, which are the roto-translational[1], vibrational and electronic temperatures respectively. What constitutes an adequate description of the energy distribution is subjective. For the purpose of simulating flow fields around hypersonic vehicles, an *adequate* model is the one that allows an accurate prediction of convective and radiative heating of the surface. More detailed models tried to describe the vibrational energy of each species with a different vibrational temperature. Multivibrational temperature models accuracy relies on the availability of experimental data related to the species relaxation time, and so constitute a far more complicated way, and yet not-so-adequate to describe the roto-translational temperature [5].

Park presented in 1987 a two-temperature model based on the observed [13]:

- fast energy exchange between translational modes of free electrons and the vibrational mode of N_2;
- fast equilibration of the lower electronic states of heavy particles (molecules, atoms, ions) at the temperature associated with the ground electronic state.

In the 2-T model, the translational and rotational energies are treated as one equilibrium energy mode specified by a roto-translational temperature T_{rt}. The electron translation, electronic excitation, and species vibrational energies are treated as one nonequilibrium energy mode represented by the electron-electronic-vibrational temperature T_{ev}. The 2-T model is obtained by combining equations 5 and 6 in one.

Vibrational-Electronic Energy conservation

$$\frac{\partial}{\partial t}\rho e_{ev} + \frac{\partial}{\partial x^j}\rho e_{ev} u^j = -p_e\frac{\partial u^j}{\partial x^j} + \frac{\partial}{\partial x^j}\left[(\eta_v + \eta_e)\frac{\partial T_{ev}}{\partial x^j}\right] + \frac{\partial}{\partial x^j}\left(\rho\sum_{s=1}^{11} h_{ev,s} D_s \frac{\partial y_s}{\partial x_j}\right) + \dot{Q}_{v-t} + \dot{C}_{h-e}(T_{ev}) - \dot{I}^e + \sum_{s=1}^{N_{mol}} \dot{w}_s \hat{D}_s + \dot{Q}_{rad} \quad (8)$$

Where the vibrational-electronic energy (property of the mixture) and vibrational-electronic enthalpy for species s per unit mass are :

$$e_{ev} = e_v + e_e$$
$$h_{ev,s} = h_{v,s} + h_{e,s}$$

4. Chemical-kinetic models

The mass rate production of species s per unit volume appearing in 8 and 5 is expressed as [5, 15]

$$\dot{w}_s = M_s \sum_{r=1}^{N_r}(\beta_{s,r} - \alpha_{s,r}) \cdot \left[k_{f,r}\prod_{s=1}^{11}\left(\frac{\rho_s}{M_s}\right)^{\alpha_{s,r}} - k_{b,r}\prod_{s=1}^{11}\left(\frac{\rho_s}{M_s}\right)^{\beta_{s,r}}\right] \quad (9)$$

Where N_r is the total number of reactions taking place, $\alpha_{s,r}$ and $\beta_{s,r}$ are the stoichiometric coefficients for reactants and products in the r reaction respectively. $k_{f,r}$ and $k_{b,r}$ are the forward and backward coefficients for the reaction r respectively.

[1] The hypothesis behind the coupling of rotational and translational equilibrium is that they have a similar relaxation time, and small compared to the vibrational and electronic ones.

4.1. Chemical-vibrational coupling

In the literature, two types of chemical-vibrational coupling have been proposed: preferential and non-preferential dissociation. The first claims that dissociation of molecular species is obtained more easily when they are vibrationally excited. Despite so, when the conditions are highly energetic (very high velocities) the dissociation may occur at lower levels, in a non-preferential way. The present work is devoted to comparing four preferential chemical-vibrational couplings models: Park-87, Park-91, Gupta and Dunn-Kang.

4.2. Reaction rates

The forward rate coefficients of the chemical reaction for all four models is obtained by the Arrhenius formula [1]

$$k_{f,r} = C_{f,r} T_d^{n_{f,r}} exp\left(\frac{-E_{f,r}}{kT_d}\right) \tag{10}$$

Where $C_{f,r}$, $n_{f,r}$ and the activation energy $E_{f,r}$ divided by the Boltzmann constant k are kinetic parameters established empirically for a set of chemical reactions involving the eleven species of air. The temperature T_d is a dummy variable for the rate-controlling temperature, and in all four cases is assumed to be the geometric average of the roto-translational and the vibrational temperatures. The temperature is heavily weighted by the vibrational temperature, because of the preferential concept, in the following way:

$$T_d = \sqrt{TT_v} \tag{11}$$

Park-87 and Park-91 models prescribe a backward rate coefficient that depends on the equilibrium constant of the reaction K_r

$$k_{b,r} = \frac{k_{f,r}(T)}{K_r} \tag{12}$$

The equilibrium constants of Park-87 and Park-91 models are evaluated by the following curve fits of temperature, respectively:

$$\ln(K_r) = A + B\ln(Z) + CZ + DZ^2 + EZ^3$$
$$\ln(K_r) = A/Z + B + C\ln(Z) + DZ + EZ^2$$

Where $Z = 10^4/T$, and coefficients A, B, C, D, E are parameters of each chemical reaction available in [13, 14] respectively. The backward rate coefficients in Dunn-Kang model are obtained by Arrhenius form [4]

$$k_{b,r} = C_{b,r} T_d^{n_{b,r}} exp\left(\frac{-E_{b,r}}{kT_d}\right) \tag{13}$$

For velocities below 8 km/s, the backward rate coefficients of Gupta model are evaluated by Arrhenius formula 10. For higher velocities, the backward rate coefficients of Gupta model are obtained from the equilibrium constants [6]:

$$k_{b,r} = \frac{k_{f,r}(T_d)}{K_r(T_d)} \tag{14}$$

Generally speaking, the chemical-kinetic models are defined by a set of elementary reactions, equilibrium constants and relative parameters for each reaction, forward and backward coefficients formulations, and the rate-controlling temperature. All four models presented share the same rate-controlling temperature and the same form of the forward rate coefficient. They hence differ in the set of elementary equations among the eleven species, relative parameters to define the equilibrium constant in addition to the backward rate coefficient formulation.

5. Comparison

A comparative study by Wang [18] of the the four kinetic models is now presented and commented. The comparison was carried out numerically with a in-house code developed by Wang et al. in [17]. The test-case studied is the Apollo command module, a typical geometry for re-entry vehicles. The Apollo typical flow features are visible in Fig.1. The free stream conditions, which are taken from the AS-202 flight test [16], are listed in Tab.1.

U (m/s)	Ma	AoA (deg)	H (km)
6210	20.5	18.4	67.3

Table 1: Freestream conditions

The grid used features 1.86 million cells, and it is visible in Fig.2. The heat flux is evaluated for the four kinetic models and plotted around the symmetry plane in Fig.3.
The heat flux at the forebody of the vehicle predicted by Gupta model is lower than the results computed with the other three models, whose heat flux shows similar behaviour. In the most

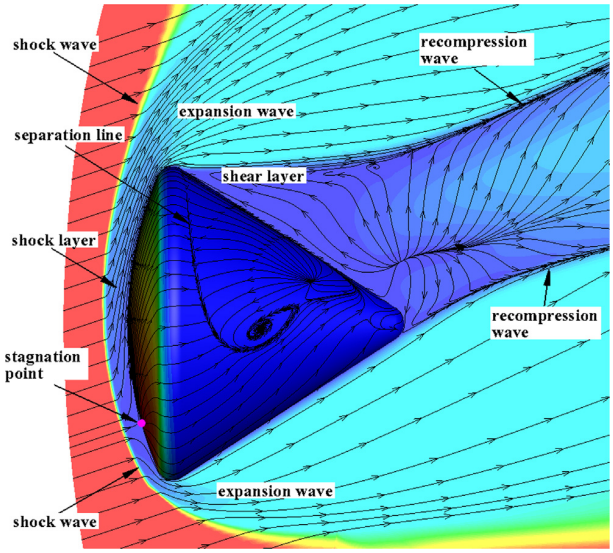

Figure 1: Apollo capsule flow features

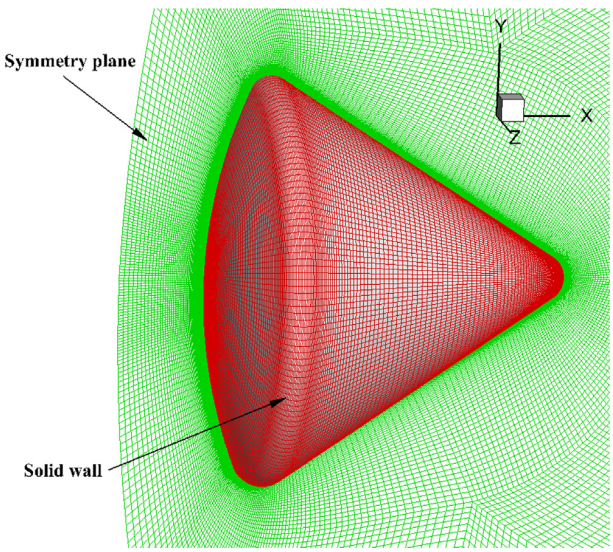

Figure 2: Grid. Windside and leeside corners are refined to capture the expansions

part of the forebody the heat fluxes predicted by Dunn-Kang model, Park-87 model and Park-91 model are nearly the same, which are about 20% higher than Gupta model. At the backbody of the vehicle, the aeroheating environment predicted by the four chemical kinetic models do not show any significant difference. The peak of heat flux is observed for all models at the same location, at the windside shoulder of the body, and are reported in Tab2. The maximum difference is about 27%.

Numerical heat flux prediction along the Apollo's surface exhibits a relatively strong sensitivity to the choice of chemical kinetic models. This difference appears to be increasing for in-

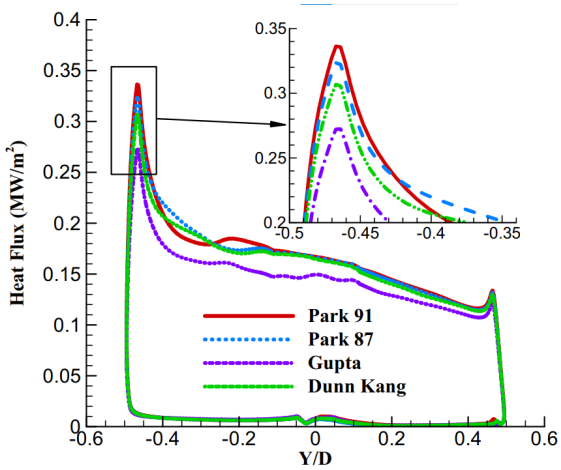

Figure 3: Heat flux profile around the symmetry plane cut

	P-87	P-91	D-K	Gupta
$\dot{q}$ (MW/m^2)	0.305	0.270	0.325	0.335

Table 2: Peak values of the heat flux for the four models

creasing complexity of the vehicle geometry and increasing Mach number[18]. To investigate the reason for these discrepancies, the chemical rates of dissociation and recombination of molecular nitrogen and molecular oxygen are compared for the four chemical-kinetic models.

$$N_2 + N_2 \rightleftharpoons 2N + N_2$$
$$O_2 + O_2 \rightleftharpoons 2O + O_2$$

If for the dissociation of N_2 there's no substantial difference (Fig.4), a sensible difference for the Gupta model is appreciated in the dissociation rate of O_2 along the whole temperature span (Fig.6). Furthermore, conspicuous differences are noticed in the recombination rates of both molecular species (Fig.5,7).

In the same work, Wang et al. [18] show, for a different test case, the influence of the choice of a chemical-kinetic model on the shock standoff distance. Also, Gnoffo et al. [5] noticed the standoff distance of the Park-87 and Dunn-Kang models was slightly different. However, due to the lack of enough flight data and a poor understanding of the chemical kinetic mechanism, it is difficult to judge which chemical kinetic model is better, and large uncertainties still exist in the chemical kinetic models.

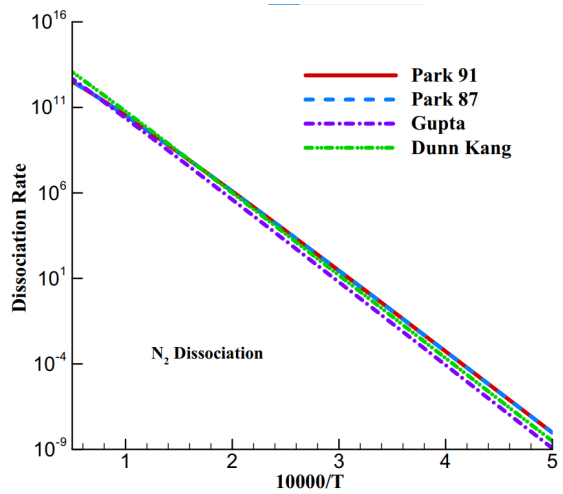

Figure 4: Dissociation rate of N_2 as function of rate temperature T_d

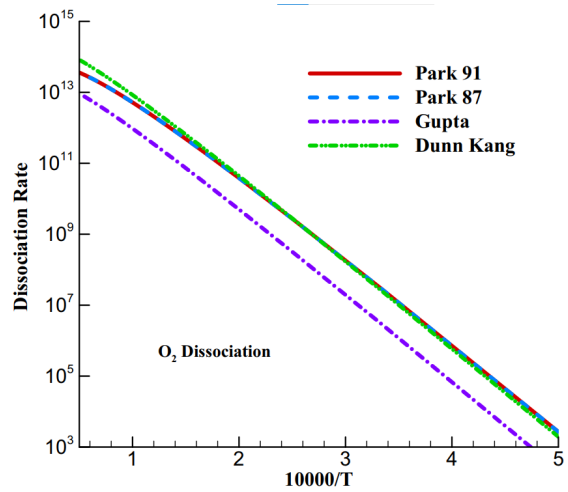

Figure 6: Dissociation rate of O_2 as function of rate temperature T_d

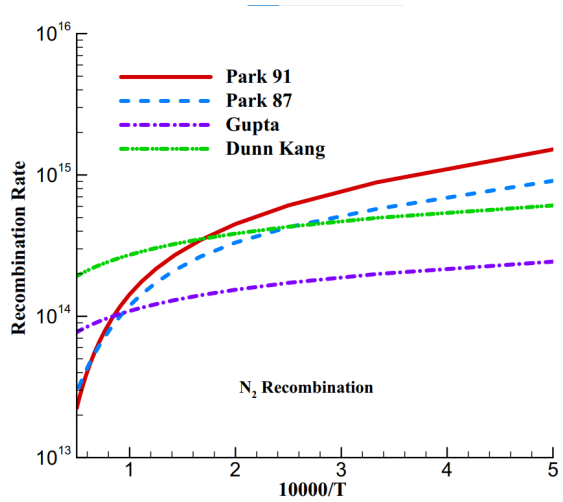

Figure 5: Recombination rate of N_2 as function of T_d

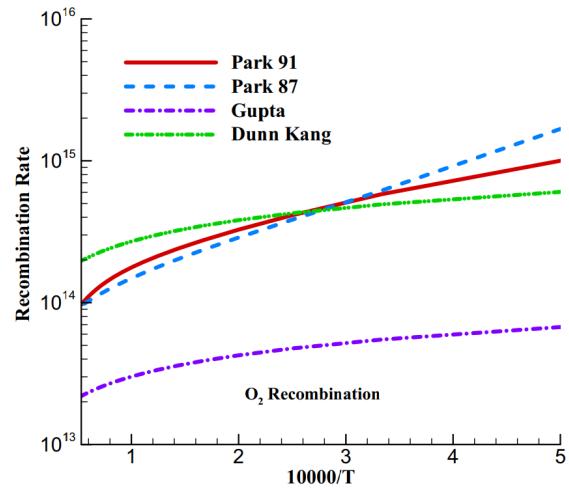

Figure 7: Recombination rate of O_2 as function of T_d

6. Concluding remarks

The conservation equations for simulating hypersonic flows in thermal and chemical nonequilibrium are presented for the three-temperature model. The two-temperature model is obtained by joining the Vibrational and Electron-Electronic Energy conservation equations. Therefore, Park's two-temperatures model of 1987 is introduced and compared with its modification of 1991, the Gupta model and the Dunn-Kang model, in terms of reaction rates. To assess the differences, the test case of Apollo module re-entry at $Ma = 20.5$ is considered. The heat flux at the forebody surface is noticed to be substantially affected by the choice of the chemical-kinetic model. The reason for these differences in the heat flux peaks of the four models is attributed by Wang [18] to the difference in the reaction rates for the dissociation and recombination of molecular nitrogen and molecular oxygen. Nevertheless, Gnoffo [5] and Hao [8] claim that the major impact of the choice of a kinetic model is ascribed to the ionization reactions.

In general, there is still no concrete evidence to indicate which chemical reaction model can predict better results than the other, for the simulation of hypersonic reentry flowfields. Given the lack of enough validation data and a deeper understanding of the physical mechanism of chemical kinetic models, the validity of these models is difficult to assess and large differences and un-

certainties still exist in their definition.

7. Final notes

7.1. The limits of updating empirical models

Recent works on the determination of dissociation and recombination rate coefficients [10][9][12] still hinge on modified versions of legacy models, as Park and Dunn-Kang models, based on better experimental data and computations. These updated models stand on the same basis as the legacy ones, dragging with them the poor understanding of the physical inference of those chemical-kinetic models.

7.2. Future outlook

Nowadays, the scientific community is moving towards predictive models to control natural phenomena. In this framework, model calibration acquires a critical role in its validation. The incomplete understanding of the physical implication of a model makes its uncertainty unknown and its calibration inaccurate, ultimately leading to results with unknown reliability outside the competence of the specific experimental case. That is why it is of essential importance that uncertainty assessment is led during the construction of the empirical model, starting from the assumptions about the experimental data and post-processing [2][3].

References

[1] FG Blottner. Viscous shock layer at the stagnation point with nonequilibrium air chemistry. *AIAA Journal*, 7(12):2281–2288, 1969.

[2] Anabel del Val. *Bayesian calibration and assessment of gas-surface interaction models and experiments in atmospheric entry plasmas*. PhD thesis, Institut polytechnique de Paris; Ecole Polytechnique (Palaiseau, France . . . , 2021.

[3] Anabel Del Val and Olivier Chazot. Stochastic determination of thermal reaction rate coefficients for air plasmas. *The Journal of Chemical Physics*, 159(6), 2023.

[4] Michael G Dunn and S Kang. Theoretical and experimental studies of reentry plasmas. Technical report, NASA, 1973.

[5] Peter A Gnoffo. *Conservation equations and physical models for hypersonic air flows in thermal and chemical nonequilibrium*, volume 2867. National Aeronautics and Space Administration, Office of Management . . . , 1989.

[6] Roop N Gupta, Jerrold M Yos, Richard A Thompson, and Kam-Pui Lee. A review of reaction rates and thermodynamic and transport properties for an 11-species air model for chemical and thermal nonequilibrium calculations to 30000 k. 1990.

[7] C Frederick Hansen and Steve P Heims. A review of the thermodynamic, transport, and chemical reaction rate properties of high-temperature air. 1958.

[8] Jiaao Hao, Jingying Wang, and Chunhian Lee. Numerical study of hypersonic flows over reentry configurations with different chemical nonequilibrium models. *Acta Astronautica*, 126:1–10, 2016.

[9] Bernd Helber, Alessandro Turchi, and Thierry E Magin. Determination of active nitridation reaction efficiency of graphite in inductively coupled plasma flows. *Carbon*, 125:582–594, 2017.

[10] Jae Gang Kim and Sung Min Jo. Modification of chemical-kinetic parameters for 11-air species in re-entry flows. *International Journal of Heat and Mass Transfer*, 169:120950, 2021.

[11] J-H Lee. Basic governing equations for the flight regimes of aeroassisted orbital transfer vehicles. In *19th Thermophysics Conference*, page 1729, 1984.

[12] Francesco Panerai and Olivier Chazot. Characterization of gas/surface interactions for ceramic matrix composites in high enthalpy, low pressure air flow. *Materials Chemistry and Physics*, 134(2-3):597–607, 2012.

[13] Chul Park. Assessment of a two-temperature kinetic model for dissociating and weakly ionizing nitrogen. *Journal of*

Thermophysics and Heat Transfer, 2(1):8–16, 1988.

[14] Chul Park, JOHN HOWE, RICHARD JAFFE, and GRAHAM CANDLER. Chemical-kinetic problems of future nasa missions. In *29th Aerospace Sciences Meeting*, page 464, 1991.

[15] GSR Sarma. Physico–chemical modelling in hypersonic flow simulation. *Progress in Aerospace Sciences*, 36(3-4):281–349, 2000.

[16] Louis MG Walpot, Michael J Wright, Peter Noeding, and Ferry Schrijer. Base flow investigation of the apollo as-202 command module. *Progress in aerospace sciences*, 48:57–74, 2012.

[17] Xiaoyong Wang, Chao Yan, Weilin Zheng, Kang Zhong, and Yunfei Geng. Laminar and turbulent heating predictions for mars entry vehicles. *Acta Astronautica*, 128:217–228, 2016.

[18] XY Wang, Chao Yan, YK Zheng, and EL Li. Assessment of chemical kinetic models on hypersonic flow heat transfer. *International Journal of Heat and Mass Transfer*, 111:356–366, 2017.

Regions with chemical and thermal nonequilibrium	
Region	Aerothermal phenomenon
A	Chemical and thermal equilibrium
B	Chemical nonequilibrium with thermal equilibrium
C	Chemical and thermal nonequilibrium

Chemical species in high-temperature air		
Region	Air chemical model	Species present
I	2 species	O_2, N_2
II	5 species	O_2, N_2, O, N, NO
III	7 species	$O_2, N_2, O, N, NO, NO^+, e^-$
IV	11 species	$O_2, N_2, O, N, NO, O_2^+, N_2^+, O^+, N^+, NO^+, e^-$

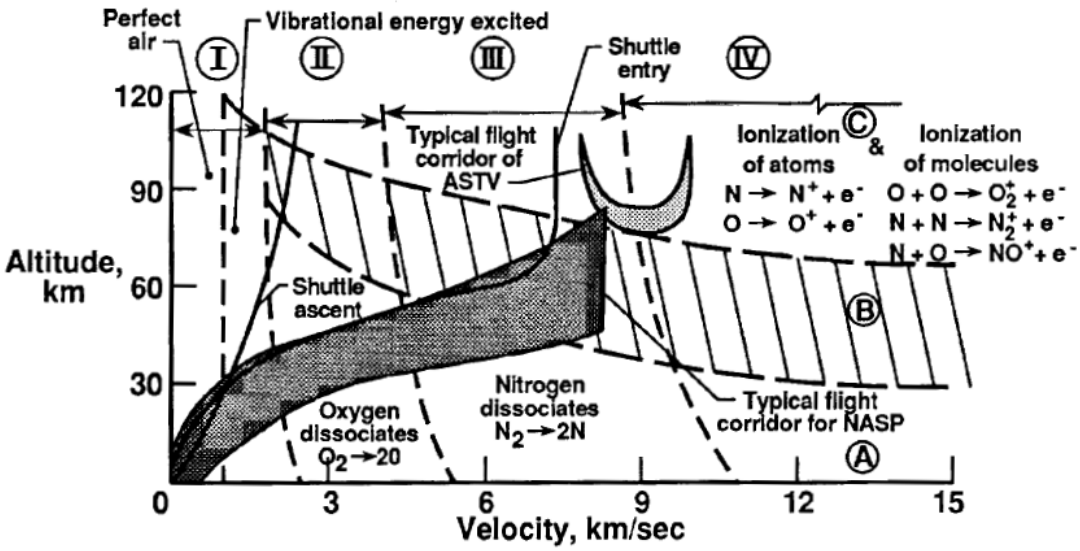

Figure 8: Chemistry of the stagnation region for a sphere of 30.5 cm radius (taken from Hansen [7])